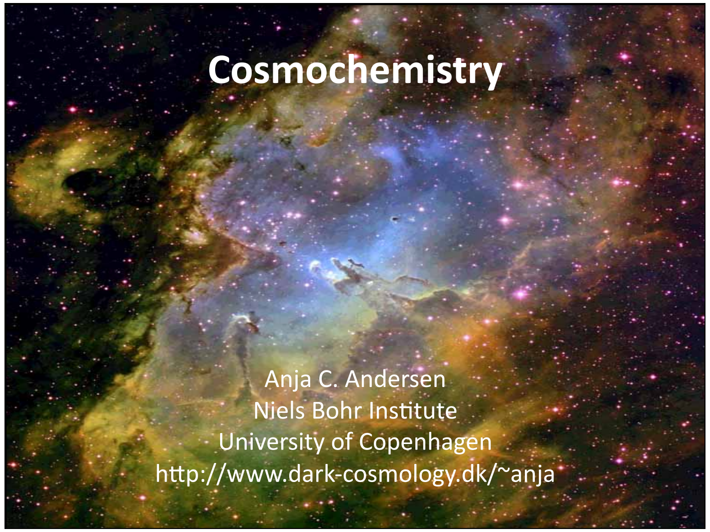
Cosmochemistry
Anja C. Andersen
Niels Bohr Institute
University of Copenhagen
http://www.dark-cosmology.dk/~anja

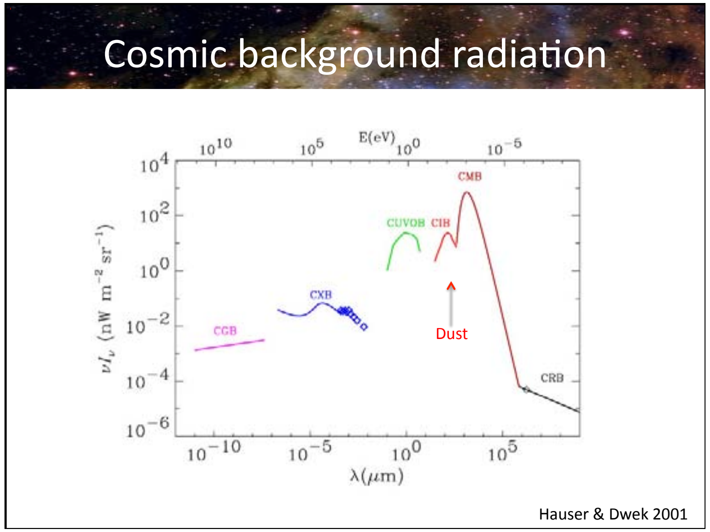
Cosmic background radiation
E(eV)
10^10
10^5
10^0
10^-5
10^4
10^2
10^0
10^-2
10^-4
10^-6
νI_ν (nW m^-2 sr^-1)
CMB
CUVOB
CIB
CXB
CGB
CRB
Dust
10^-10
10^-5
10^0
10^5
λ(μm)
Hauser & Dwek 2001

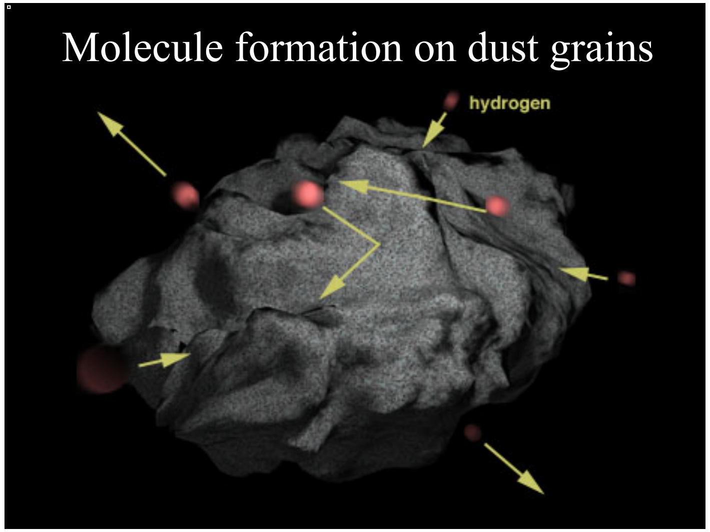
Molecule formation on dust grains
hydrogen

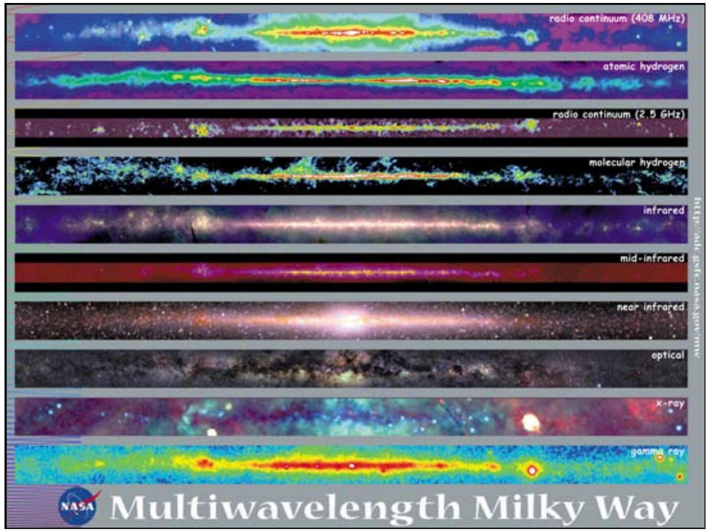
radio continuum (408 MHz)
atomic hydrogen
radio continuum (2.5 GHz)
molecular hydrogen
infrared
mid-infrared
near infrared
optical
x-ray
gamma ray
Multiwavelength Milky Way

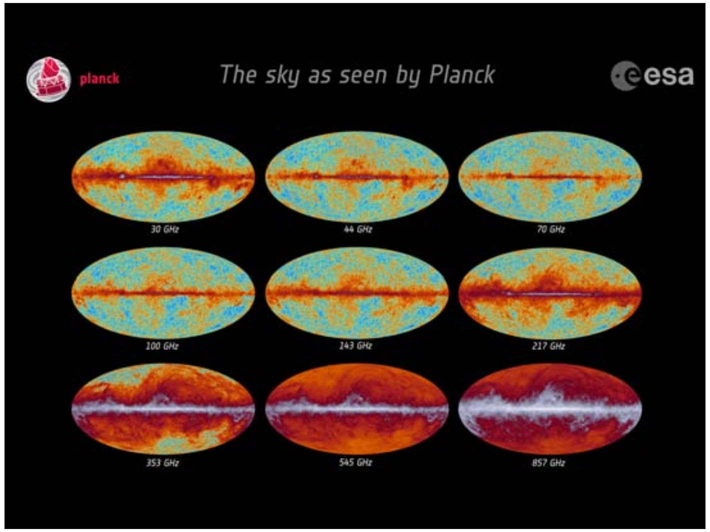

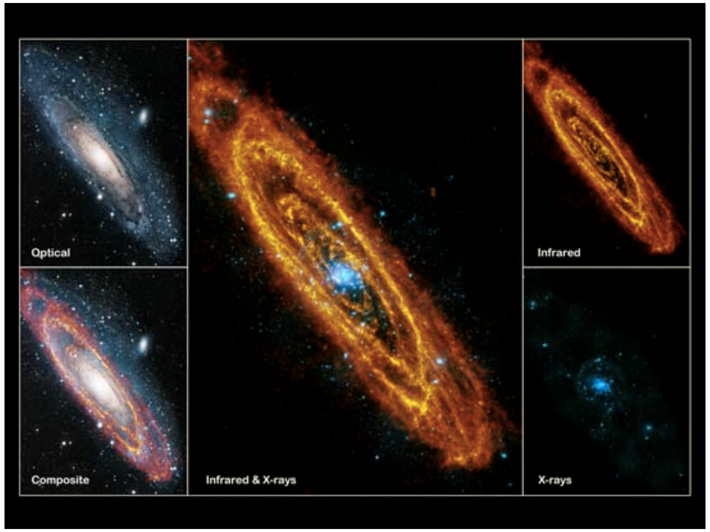

Gas-phase element depletions in the interstellar medium

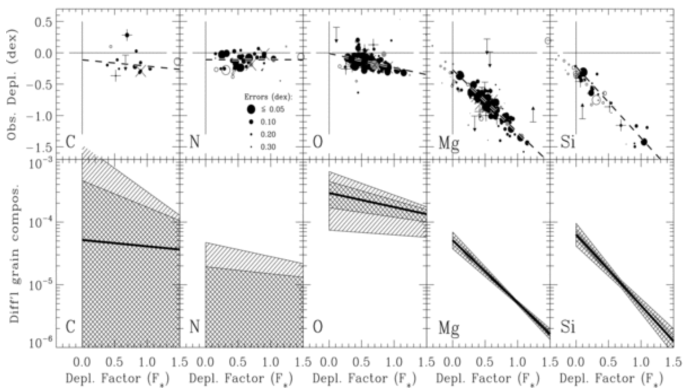

Jenkins 2009

Concept of dust depletion

The depletion of an element *X* in the ISM is defined in terms of (a logarithm of) its reduction factor below the expected abundance relative to that of hydrogen if all of the atoms were in the gas phase,

$$[X\text{gas/H}] = \log\{N(X)/N(\text{H})\} - \log(X/\text{H})_\odot$$

which is based on the assumption that solar abundances $(X/\text{H})_\odot$ are good reference values that truly reflect the underlying total abundances. In this formula, $N(X)$ is the column density of element *X* and $N(\text{H})$ represents the column density of hydrogen in both atomic and molecular form, i.e., $N(\text{H I}) + 2N(\text{H}_2)$. The missing atoms of element *X* are presumed to be locked up in solids within dust grains or large molecules that are difficult to identify spectroscopically, with fractional amounts (again relative to H) given by

$$(X_{\text{dust}}/\text{H}) = (X/\text{H})_\odot(1 - 10^{[X\text{gas/H}]}).$$

Jenkins 2009

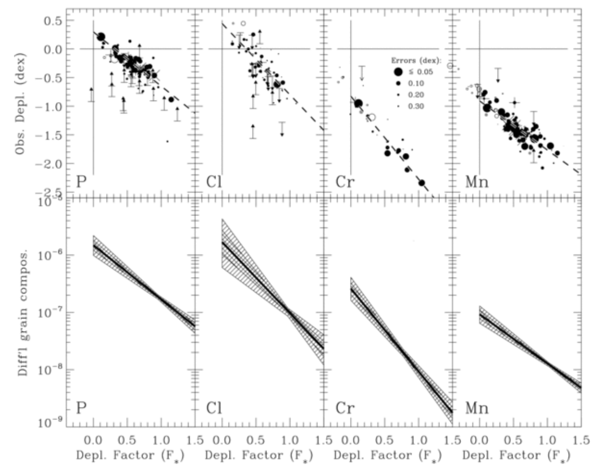

Jenkins 2009

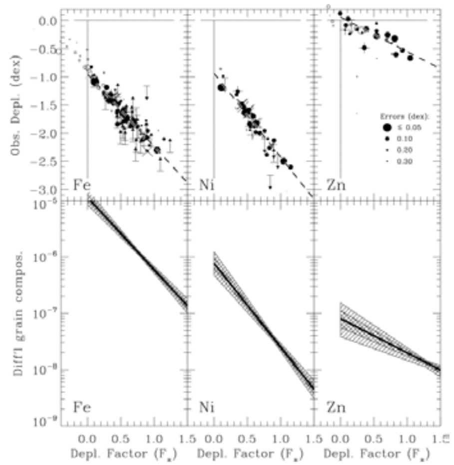

Jenkins 2009

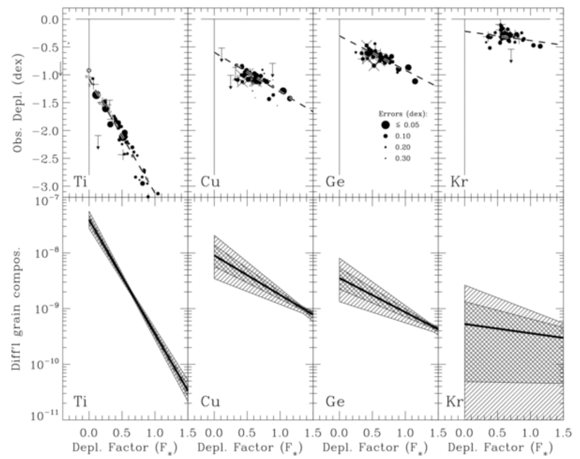

Jenkins 2009

The Galactic Extinction Curve

Extinction curves measure the difference in emitted and observed light.
Traditionally measured by comparing two stars of the same spectral type.

Galactic Extinction - empirically determined:
$\langle A(\lambda)/A(V) \rangle = a(\lambda^{-1}) + b(\lambda^{-1})/R_V$ (Cardelli et al. 1999)

- Bump at 2175 Å (4.6 μm^{-1})
- R_V : Ratio of total to selective extinction in the V band
- Mean value is R_V = 3.1 (blue)
- Low value: R_V = 1.8 (green) (Udalski 2003)
- High value: R_V = 5.6-5.8 (red) (Cardelli et al. 1989; Fitzpatrick et al. 1999)

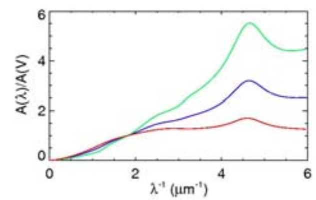

Graph from Eliasdottir et al. (2006)

Extinction

Extinction = Absorption + Scattering

$$I_{in} = I_{out}\, e^{-\tau}$$

$$\tau = N\sigma L$$

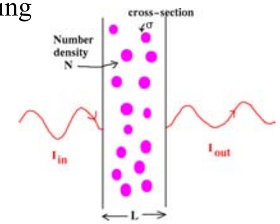

Q_{ext} = extinction effeciency factor
= cross section per unit area = σ/A

Q_{ext} (atoms) < Q_{ext} (molecules) < Q_{ext}(dust)

Other nearby galaxies

- **LMC**: Smaller bump and steeper rise into the UV (Nandy et al. 1981)
- **SMC**: No bump, well fitted by A(λ) ∝ 1/ λ (Prevót et al. 1984)
- **M31**: Average Galactic extinction law (Bianchi et al. 1996)

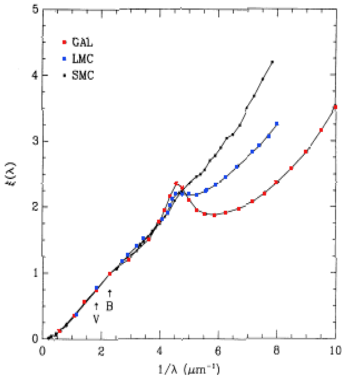

Graph from Pei (1992)

Cosmic Dust - ”basic facts”

- 1/5 of the part of the Milky Way consisting of stars, planets and other “baryonic matter” is present as gas and dust. Of this 1/5 then 99% is gas and 1% is dust.
- Smoke particles consisting of C, O, Si, Mg, Al, Fe.

General dust facts

- Nucleation – requires supersaturation pressure

$$S = \frac{P_{mon}}{P_{sat}(T_d)}$$

- Change of dust mass:
  - Growth – when smaller dust particle increase its size
  - Destruction – when dust grain evaporates into gas phase
- No change of dust mass:
  - Shattering – when larger grain is spilt into smaller dust grains
  - Coagulation – smaller grains form larger grains
- Elements available for dust: C, O, Mg, Si, S and Fe

Dust effects

- Dust drives the mass loss of AGB stars.
- Dust is an important coolant during star formation, possibly essential for low mass star formation.
- Dust plays a crucial role for molecule formation in the ISM.
- Dust is an ingredient of planet formation.
- Dust determine "the weather" of BDs.
- Dust can be really irritating for certain observations!

History of the Universe

- Big Bang formed H (75%), He (25%), (Li, B, Be) ➡ No dust!
- Heavier elements are produced in stars.
- The abundance (by mass) today is H (74%), He (25%), all the rest ~ 1%

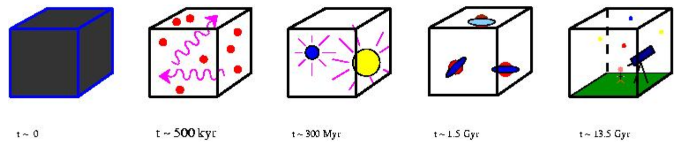

Relative abundance of the elements today

For each Au atom

~ 1 million Fe

~ 30 million C

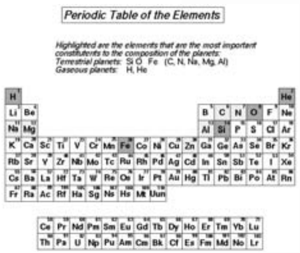

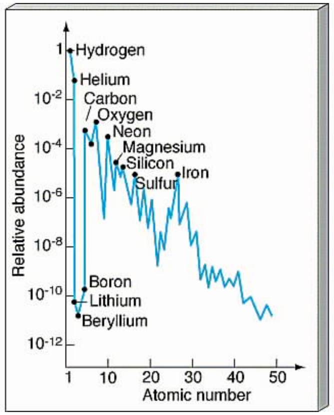

Stellar evolution

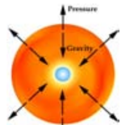

Gas and radiation pressure vs. gravity

Processed elements are blown away

Degenerate e- or n pressure vs. gravity

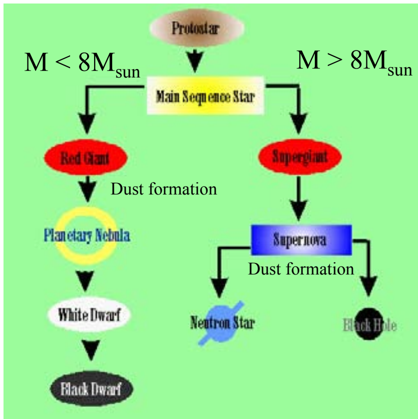

Recycling

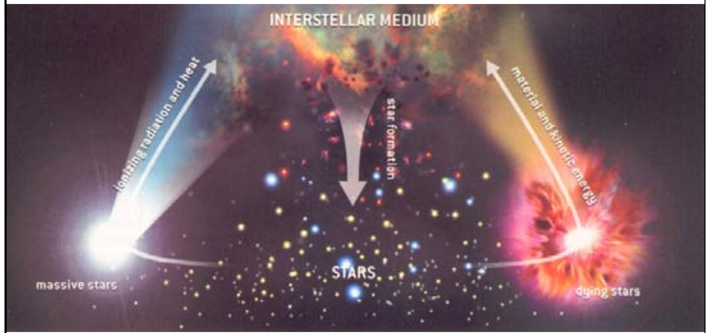

Extraterrestrial samples

- Meteorites (from asteroids, Mars and the Moon).
- Lunar samples (returned by Apollo and Luna)
- Micrometeorites.
- Interplanetary dust particles (IDPs)
- Samples returned from comets (STARDUST)
- Samples from the Sun (Genesis)

Meteorites

Meteorites have proven difficult to classify, but the three broadest groupings are stony, stony iron, and iron

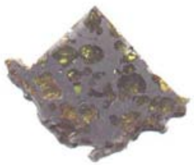

Chondrites

Chondrites – 85.7% of falls – age 4.55 billion years – pristine samples of early solar system although in many cases their properties have been modified by thermal metamorphism or icy alteration.

Subgroups: Enstatites contain the most refractory elements and are believed to have formed in the inner solar system. Ordinary chondrites, being the most common type containing both volatile and oxidized elements, are thought to have formed in the inner asteroid belt. Carbonaceous chondrites, which have the highest proportions of volatile elements and are the most oxidized, are thought to have originated in even greater solar distances.

Chondrules


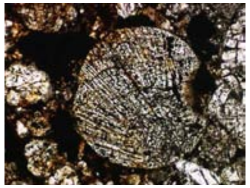

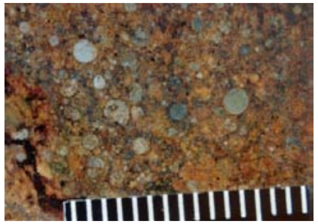

Achondrites

Achondrites – 7.1% of falls - are also stony meteorites, but they are considered differentiated or reprocessed matter. They are formed by melting and recrystallization on or within meteorite parent bodies; as a result, achondrites have distinct textures and mineralogies indicative of igneous processes.

Subgroups: HED group thought to originate from asteroid Vesta. SNC group thought to originate from Mars. Aubrites which maybe originates from asteroid Nysa. Ureilites which maybe represents a c-type astroide.

Stony iron meteorites

Stony iron meteorites – 1.5% of falls.

Subgroups: Pallasites composed of olivine enclosed in metal. Mesosiderites appear to be a surface regolith that has been stirred up and fused by repeated impacts.

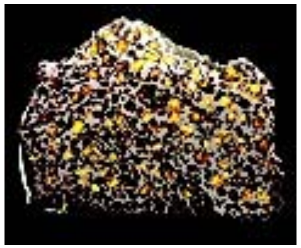


Iron meteorites

Iron meteorites – 5.7% of falls - are classified into thirteen major groups and consist primarily of iron-nickel alloys with minor amounts of carbon, sulfur, and phosphorus. These meteorites formed when molten metal segregated from less dense silicate material and cooled.


Kamacite and teanite

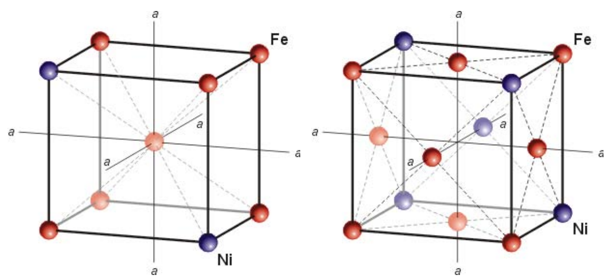

Iron and nickel form homogeneous alloys at temperatures below the melting point, these alloys are taenite. At temperatures below 900 to 600°C (depending on the Ni content), two alloys with different nickel content are stable: kamacite with lower Ni-content (5 to 15% Ni) and taenite with high Ni (up to 50%).

Widmanstätten pattern in iron meteorites

Henbury meteorite

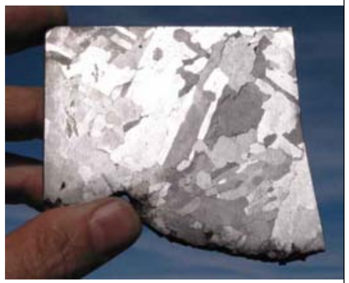

Campo meteorite

Antartica meteorites

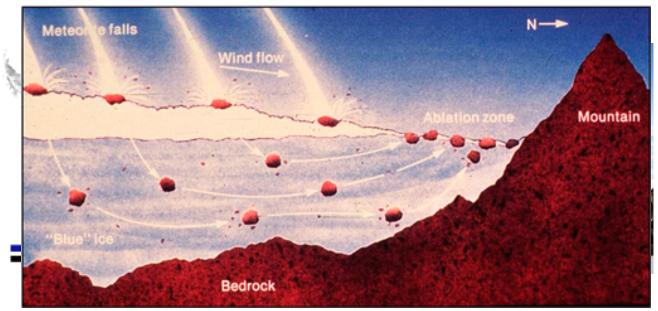

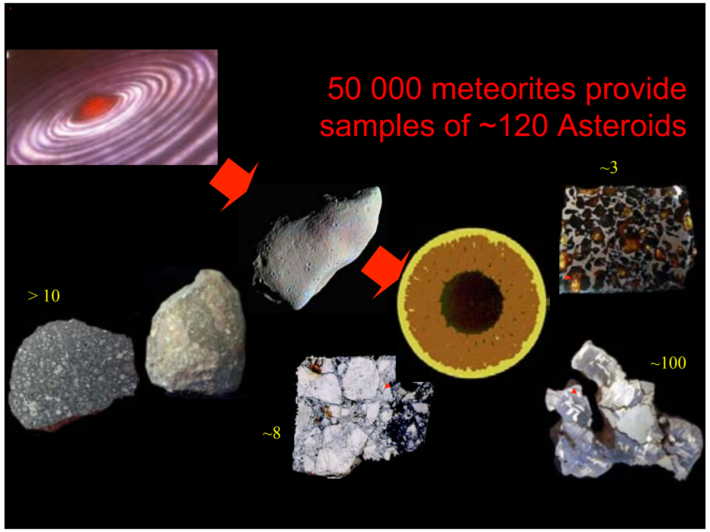

Allende meteorite

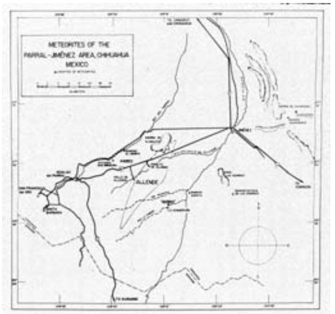

Fell in 1969 in Mexico

Allende

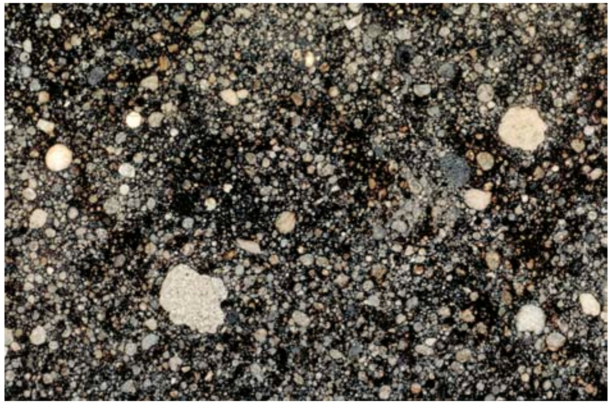

Carbonaceous chondrites

Allende Yukon Murchison

CI chondrites

CI chondrites are very rare. Out of the ~ 1000 recorded observed meteorite falls from which material is preserved, only 5 CI chondrites are known. Among the 40,000 or so meteorites collected in Antarctica, only a few are CI chondrites.

The meteorites are very fragile and decompose easily, for example, if placed in water, CI chondrites immediately begin to disintegrate. Hence, CI chondrites that are found a long time after their fall are not useful for abundance studies, as chemical information is easily altered or lost.

Table 1. Observed CI chondrite meteorite falls

Meteorite	Date of Fall	Country	Preserved Mass
Alais	15 March 1806	France	6 kg
Orgueil	14 May 1868	France	14 kg
Tonk	22 January 1911	India	10 g
Ivuna	16 December 1938	Tanzania	0.7 kg
Revelstoke	31 March 1965	Canada	$\leq$1g

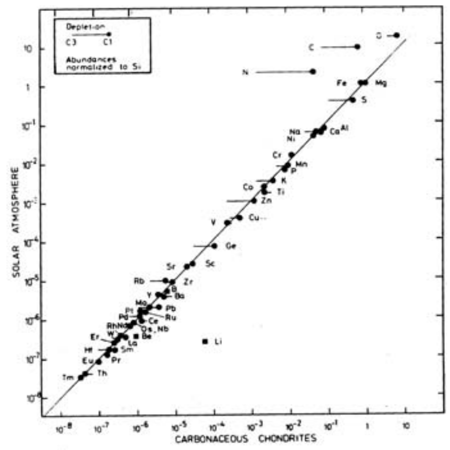

Figure 7.7. Abundances in the Solar Atmosphere Compared with those in C1 and C3 Carbonaceous Chondrites. Courtesy H. Holweger and International Astronomical Union.

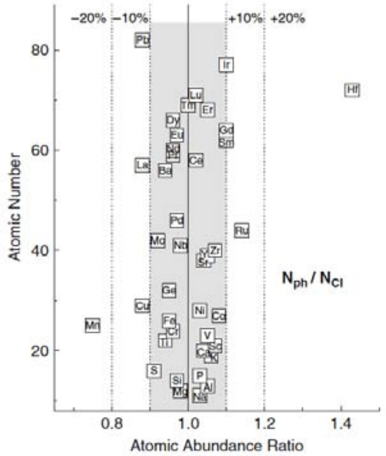

Fig. 3. The photospheric/CI chondritic abundance ratios for 39 elements that are well determined for the solar photosphere. The grey-shaded region shows agreement within 10%

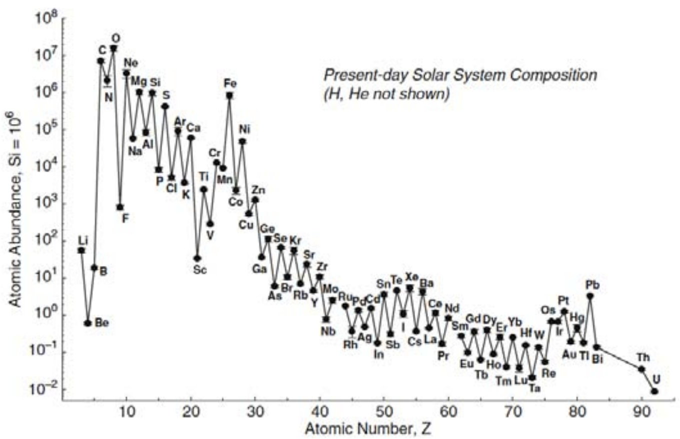

Presolar grains

In 1987 it was discovered that primitive meteorites contain small quantities of presolar grains.

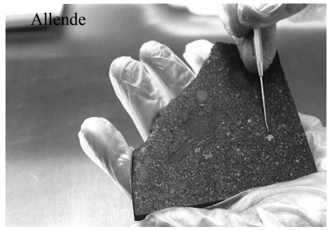

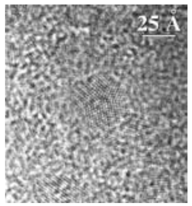

Diamond

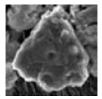

SiC

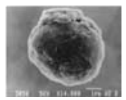

Graphite

Al_2O_3

Atomic lattice distance and bonds

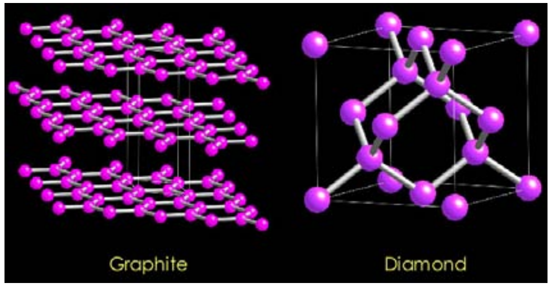

Graphite = carbon atoms

Diamond = carbon atoms

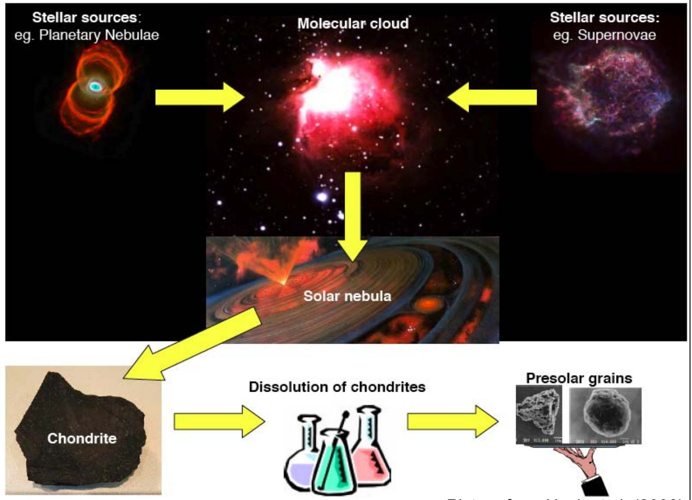

Picture from Heck et al. (2006)

Types of presolar grains extracted from meteorites by acid dissolution

Type	Abundance (parts per million)	Size
Nanodiamond (C)	1400	2 nanometers
Silicon carbide (SiC)	14	0.1-20 micrometers
Graphite (C)	10	1-20 micrometers
Carbides of titanium, zirconium, molybdenum, ruthenium, and iron, and iron-nickel metal	Small grains inside presolar graphite	5-220 nanometers
Silicon nitride (Si_3N_4)	>0.002	About 1 micrometer
Corundum (Al_2O_3)	About 0.05	0.5-3 micrometers
Spinel ($MgAl_2O_4$)	<0.05	0.1-3 micrometers
Hibonite ($CaAl_{12}O_{19}$)	0.002	2 micrometers
Titanium dioxide (TiO_2)	One grain	About 1 micrometer

Nittler 2003

Nano-diamonds

Nano-diamonds precipitate as a cloudy white gel from acidic solution but they completely “dissolve” in basic solution.

Photo courtesy of Roy S. Lewis

Extracting of presolar grains

The steps of the chemical isolation procedure and the resulting presolar grain size- and density-fractions from the Murchison meteorite.

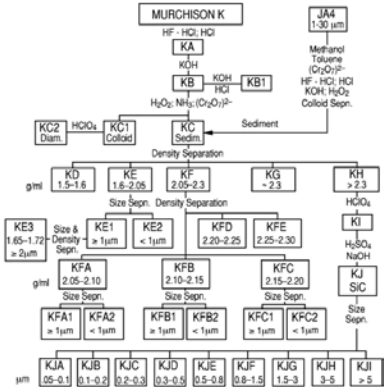

Amari et al. 1994

Nobel gas in presolar diamond

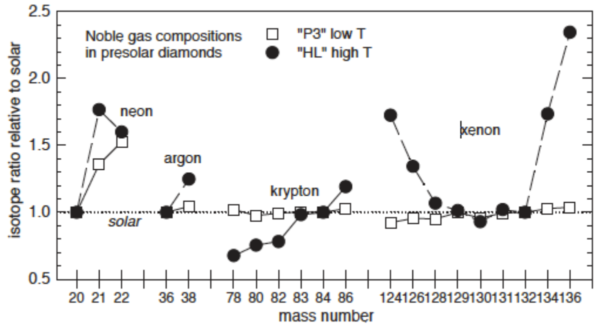

Lodders & Amari 2005

Presolar SiC

Secondary electron images of SiC grains from the Murchison meteorite. Larger grains such as these shown are relatively rare. The pitted surface structure is common for SiC grains, and most likely due to the harsh chemical treatments during the extraction from meteorites. The $^{12}C/^{13}C$ ratio of the left grain is 55 (cf. solar=89). Right a SiC grain with a smooth surface. The $^{12}C/^{13}C$ ratio of this grain is 39.

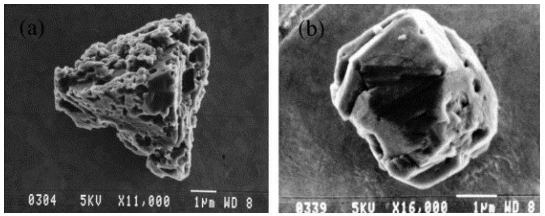

Noble gas components in SiC grains

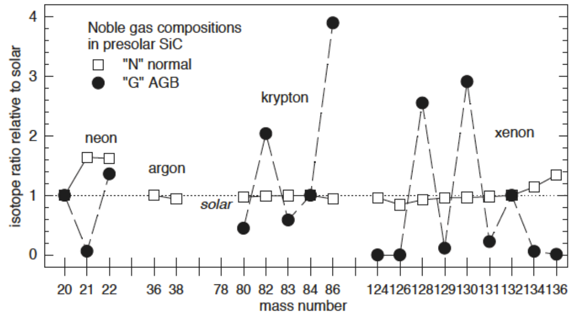

Noble gas components in aggregates of SiC grains normalized to solar isotopic composition. Isotope ratios are further normalized to ^{20}Ne, ^{36}Ar, ^{84}Kr, and ^{132}Xe, respectively. The dotted line shows solar composition.

Lodders & Amari 2005

Isotopic anomalies of presolar SiC

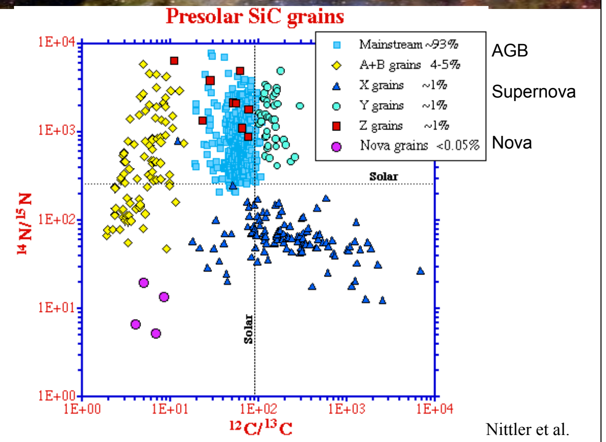

Nittler et al.

Isotopic anomalies of presolar SiC

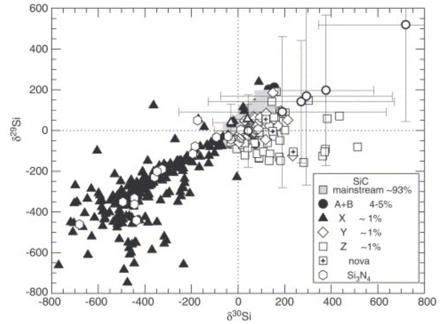

The Si-isotopes for presolar SiC grains and stars (symbols with error bars).The grains fall into distinct populations. The triangles show two determinations for the C-star IRC+10°216 (Cernicharo et al., 1986, Kahane et al., 1988). The other stellar data (circles) are for O-rich M-giants (Tsuji et al., 1994).

Lodders & Amari 2005

The δ-notation

Describes the deviation of an isotope ratio ($^iN/^jN$) of a sample from the (terrestrial) standard ratio in per-mil:

$$\delta^iN(‰)=[(^iN/^jN)_{sample}/(^iN/^jN)_{standard}-1]\times 1000.$$

Isotopic anomalies of presolar SiC

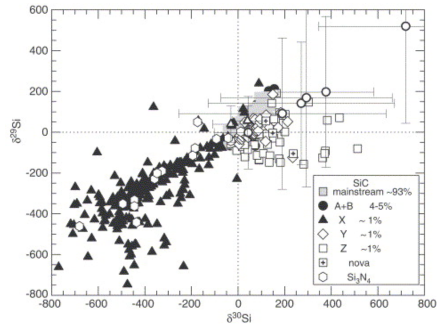

The Si-isotopes for presolar SiC grains and stars (symbols with error bars).The grains fall into distinct populations. The triangles show two determinations for the C-star IRC+10°216 (Cernicharo et al., 1986, Kahane et al., 1988). The other stellar data (circles) are for O-rich M-giants (Tsuji et al., 1994).

Lodders & Amari 2005

Isotopic anomalies of presolar SiC

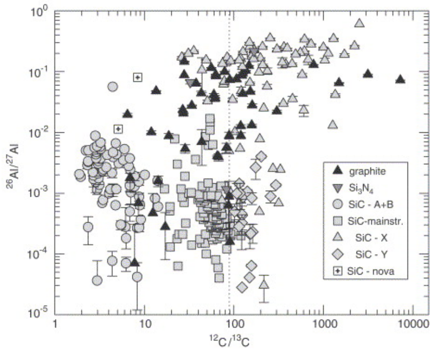

Inferred $^{26}Al/^{27}Al$ ratios versus $^{12}C/^{13}C$ ratios in SiC and low-density graphite grains. The SiC type X and graphite grains have the largest $^{26}Al/^{27}Al$.

Lodders & Amari 2005

Isotopic anomalies of presolar SiC

Trace element abundances in individual SiC grains normalized to solar abundances and Si.

Relative depletions or enrichments in Sr and Ba are most notable.

Mainstream grains are shown by black symbols, open symbols are for A+B grains, and type Y grains are shown in gray.

Abundances in two X-type SiC grains are shown in a separate panel.

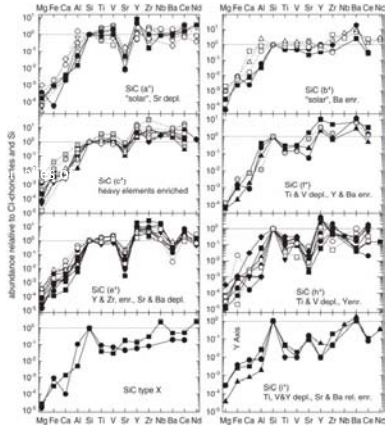

Lodders & Amari 2005

Presolar graphite

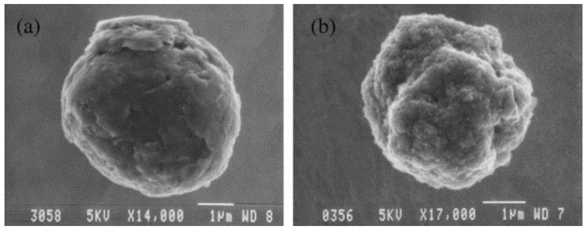

Presolar graphite grains show two morphologies: (a) a graphite grain of the "onion" type, with a layered surface structure; and (b) a graphite grain of the "cauliflower" type, which appears as aggregates of small grains.

Lodders & Amari 2005

Isotopic anomalies of presolar graphite

Carbon and N isotopes in individual graphite grains from four density fractions. Density increases in alphabetical order (E<FA<FB<FC).

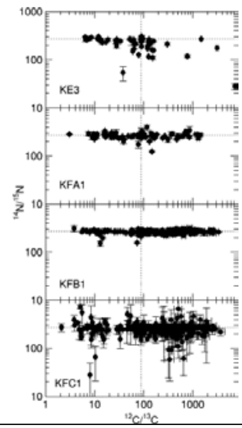

Lodders & Amari 2005

Isotopic anomalies of presolar graphite

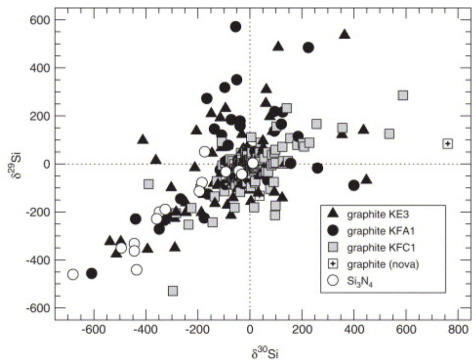

Silicon isotopes in presolar graphite grains from the low-density fractions.

Lodders & Amari 2005

Sub-grains within individual presolar grains

Sliced graphite grains contain refractory carbides (TiC, MoC as well as Fe-Ni metal). In some cases the sub-grains seem to be *nucleation sites* in other cases the appear to have been captured by growing graphite grains.

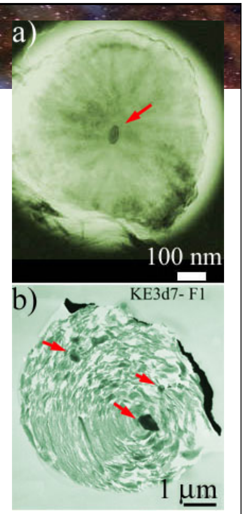

Isotopic anomalies of presolar silicate

The O-isotopes in presolar oxide and silicate grains.

Also shown are data for graphite grains from the low-density fractions KE3 (Travaglio et al., 1999) and KFA1 (Amari, unpublished); and planetary nebulae (PN), RGB, and AGB stars (Harris & Lambert, 1984, Harris et al., 1985, Harris et al., 1987 and Harris et al., 1988, Kahane et al., 1992, Lambert et al., 1986, Smith & Lambert, 1990, Wannier and Sahai, 1987). Dotted lines indicate solar ratios.

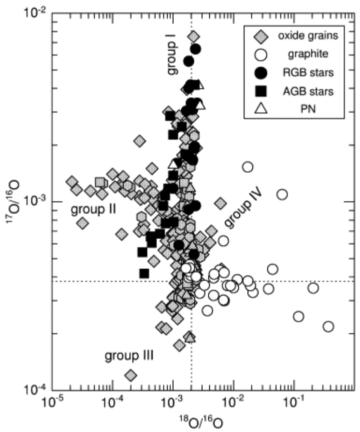

Isotopic anomalies of presolar silicate

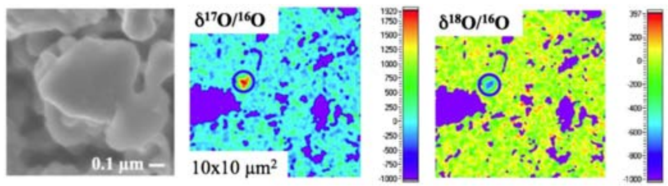

Isotopic ratio images of O calculated from isotopic raster images obtained with the NanoSIMS. An enlarged SEM picture of a presolar silicate identified from the isotopic images is also shown.

Presolar silicates are more abundant in meteorites than other presolar grains but they are small (typically 250-300 nm in diameter) and have to be detected in the presence of an overwhelming number of isotopically normal silicates of Solar System origin. Need to measure the isotopic composition of thousands and tens of thousands of grains.

Zinner et al. 2011

Mineral	Abundance (~ ppm)	Typical Size Range (μm)	Stellar Sources
Diamond	1500	0.002-0.003	SN ?
SiC	30	0.1-10	AGB (>90%) SN (1%) Novae (0.1%)
Graphite	1	0.1-10	SN (80%) AGB (<20%) Novae (2%)
Al_2O_3	0.2	0.1-5	RGB (>70%) AGB (20%) SN (<1%)
Spinel $MgAl_2O_4$	50	0.1-5	RGB (>70%) AGB (20%)
Silicates in IDPs	1000	0.1-1	RGB and AGB (>80%)
Silicates in Meteorites	100	0.1-1	RGB (>80%) AGB (10%)
Nitrides Si_3N_4	0.002	1	SN (100%)

Source: Ott & Hoppe (2005)

AGB stars are the source of almost all of SiC, Al_2O_3, spinel and silicates.

$^{12}C/^{13}C$ ratios

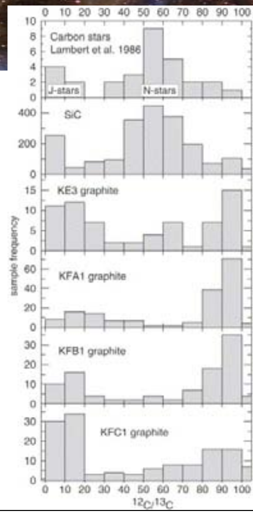

Distribution of $^{12}C/^{13}C$ ratios in presolar SiC (Hoppe et al., 1994), presolar graphite (Hoppe et al., 1995, Travaglio et al., 1999, Amari, unpublished), and in C-stars (Lambert et al., 1986). Graphite and SiC data extend to $^{12}C/^{13}C$ of several thousand. Only the observed range for C-stars is covered here.

Lodders & Amari 2005

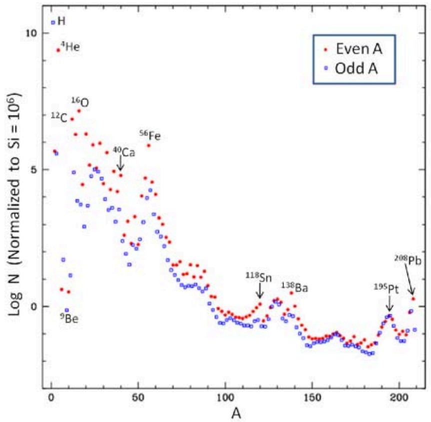

Figure 1. Solar System isotopic abundances versus mass number, *A*. Abundances are based on meteoritic samples as well as on values inferred from the solar photosphere (section 2). Values are taken from Lodders [2].

Dust from satellites

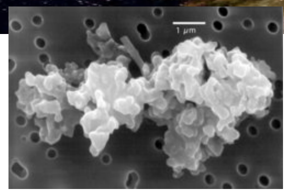

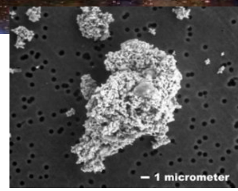

Carbon dust – sot, diamond, graphite.

Silicates – pyroxene and olivine.

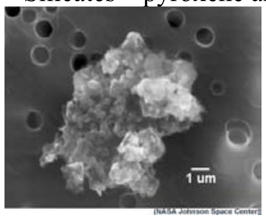

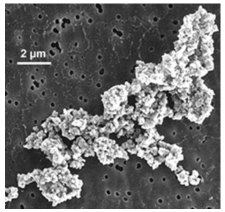

Drawing of STARDUST in action

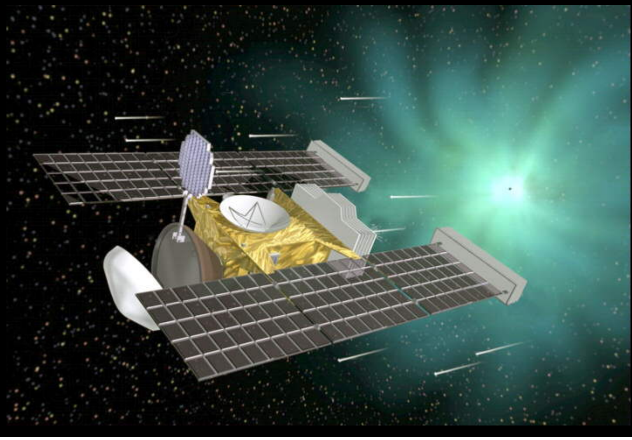

STARDUST januar 15 2006 at 2:10 am

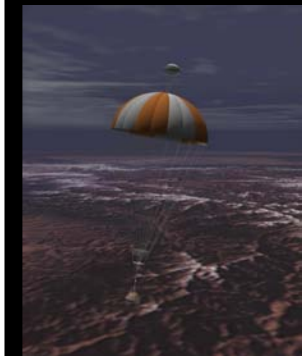

Genesis

Genesis

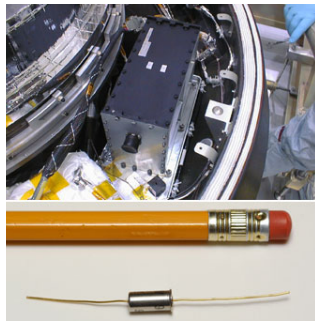

Left: Genesis staff sorting through the debris from the sample canister.
Right: a closeup of the type of accelerometer that was installed backwards, with a pencil shown for scale.

Genesis

- Genesis was a NASA sample return probe which collected a sample of solar wind and returned it to Earth for analysis.
- It was the first NASA sample return mission to return material since the Apollo Program, and the first to return material from beyond the orbit of the Moon.
- Genesis was launched on August 8, 2001, and crash-landed in Utah on September 8, 2004, after a design flaw prevented the deployment of its drogue parachute.
- The crash contaminated many of the sample collectors, and although most were damaged, many of the collectors were successfully recovered.[

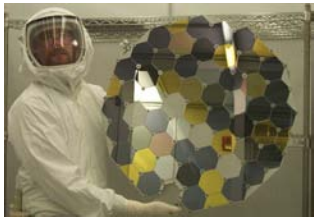

Clean room

The sample holder

Aerogel

2.5 kg brig on 2 gram of aerogel

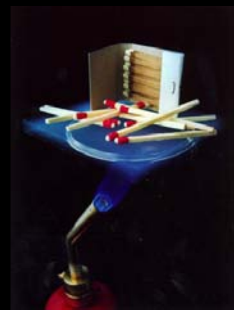


Dust in aerogel

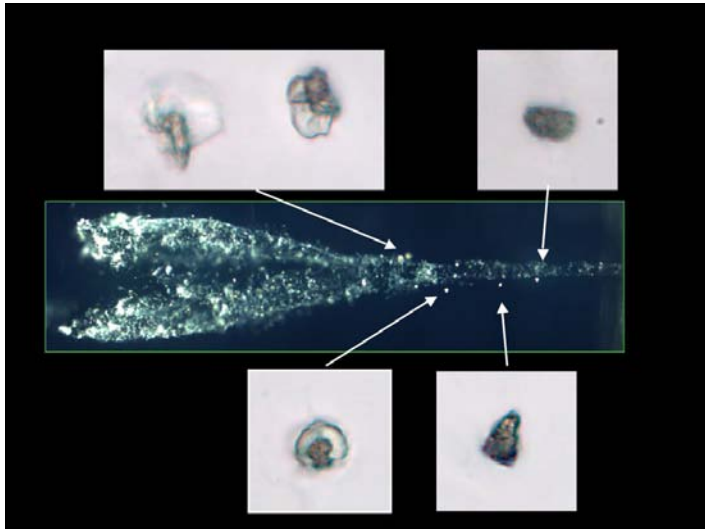

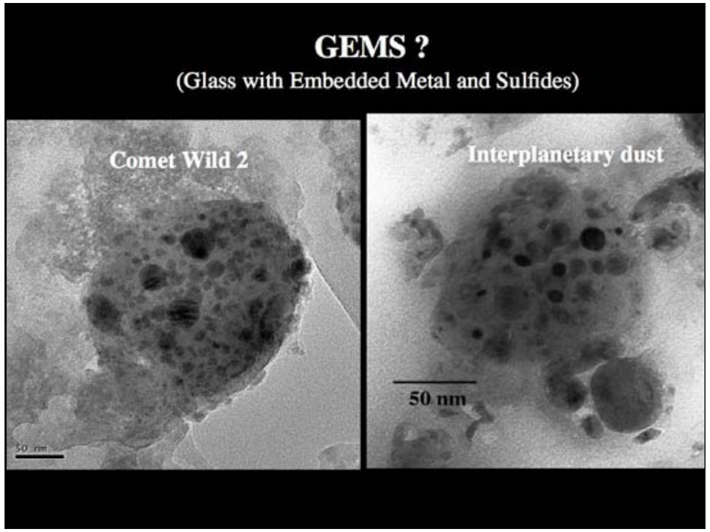
GEMS ?
(Glass with Embedded Metal and Sulfides)
Comet Wild 2
Interplanetary dust
50 nm

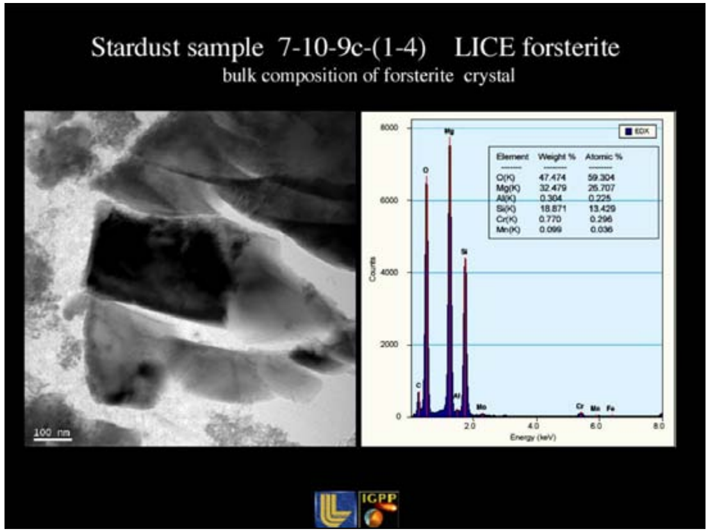
Stardust sample 7-10-9c-(1-4) LICE forsterite
bulk composition of forsterite crystal
100 nm
EDX
Element Weight % Atomic %
O(K) 47.474 59.304
Mg(K) 32.479 26.707
Al(K) 0.304 0.225
Si(K) 18.871 13.429
Cr(K) 0.770 0.296
Mn(K) 0.099 0.036
Counts
Energy (keV)
IGPP

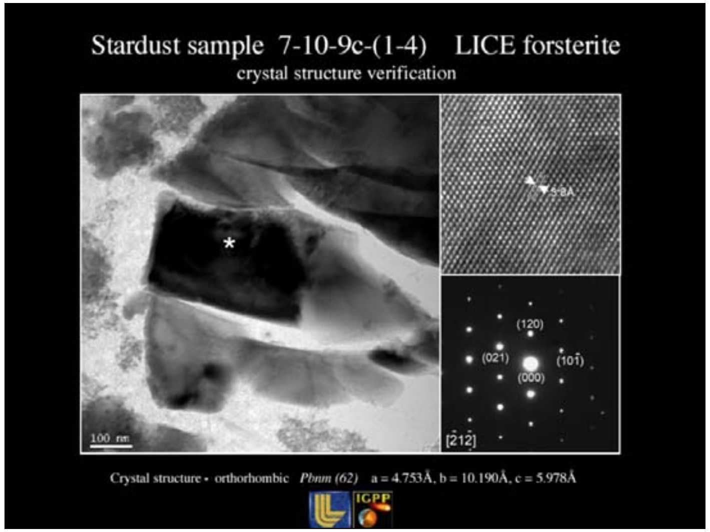

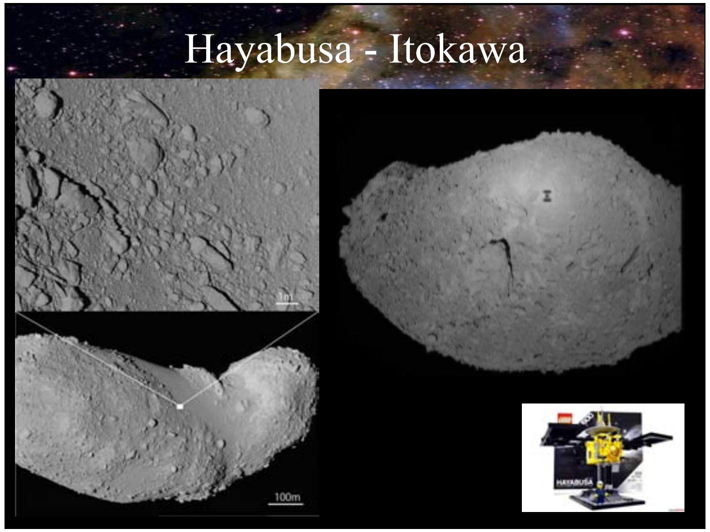

Recommended reading

- **Books:**
  - C.R. Cowley, *An Introduction to Cosmochemistry*, Cambridge University Press, 1995
  - H.Y. McSween Jr & G.R. Huss, *Cosmochemistry*, Cambridge University Press, 2010.
- **Articles:**
  - G.J. MacPherson & M.H. Thiemens, 2011, *Cosmochemistry: Understanding the Solar System through analysis of extraterrestrial materials*, PNAS 108, pp. 19130-19134.
  - E.K. Zinner, F. Moynier & R.M. Stroud, 2011, *Laboratory technology and cosmochemistry*, PNAS 108, pp. 19135-19141.
  - A.M. Davis, 2011, *Stardust in meteorites*, PNAS 108, pp. 19142-19146.
  - D.S. Burnett and Genesis Science Team, 2011, *Solar composition from the Genesis Discovery Mission*, PNAS 108, pp. 19147-19151.
  - G.J. MacPherson & A. Boss, 2011, *Cosmochemical evidence for astrophysical processes during the formation of our solar system*, PNAS 108, pp. 19152-19158.
  - T.J. McCoy, C.M. Corrigan & C.D.K. Herd, 2011, *Combining meteorites and missions to explore Mars*, PNAS 108, pp. 19159-19164.
  - K.Righter & D.P. O'Brien, 2011, *Terrestial planet formation*, PNAS 108, 19165-19170.
  - G.D. Cody, E. Heying, C.M.O. Alexander, L.R. Nittler, A.L.D. Kilcoyne, S.A. Sanford & R.M. Stroud, 2011, *Establishing a molecular relationship between chondritic and cometary organic solids*, PNAS 108, pp. 19171-19176.
  - H.Y. McSween Jr, R.L. McNutt Jr & T.H. Prettyman, 2011, *Spacecraft intrument technology and cosmochemistry*, PNAS 108, 19177-19182.

Vestas seen by DAWN

Vestas seen by Hubble and Dawn 2009

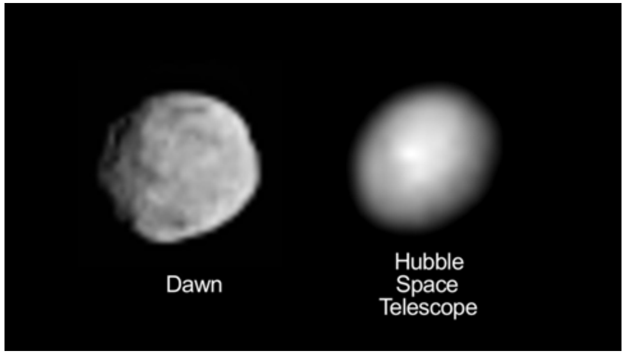

DAWN space craft details

- Dawn is a NASA space probe tasked with the exploration and study of Vesta and Ceres, the two most massive objects of the asteroid belt. Launched on September 27, 2007, the probe entered orbit around Vesta on July 16, 2011.[5][6] Dawn left Vesta on September 5, 2012, on a course for Ceres, which it is scheduled to reach in February 2015. Key Spacecraft Characteristics:
- Extensive redundancy using flight-proven assemblies from other Orbital and JPL spacecraft
- Ion propulsion system, based on the design validated on Deep Space 1
- Two 100 W (RF) traveling wave tube amplifiers, fixed 1.5 m high-gain antenna, 3 low-gain antennas, two small deep space transponders
- Solar array capable of producing more than 10 kW at Earth's distance from the Sun and more than 1 kW at Ceres's maximum distance
- Flight proven attitude control system used on Orbview, TOPEX/Poseidon ocean topography mission, and Far Ultraviolet Spectroscopic Explorer
- Simple hydrazine reaction control subsystem with two sets of six 0.9 N engines used on the Indostar spacecraft
- Command and data handling uses off the shelf components as used on the Orbview program
- Modular flight software based on design used on Orbview
- Core structure is graphite composite. Panels are aluminum core, some with aluminum facesheets and others with composite facesheets.

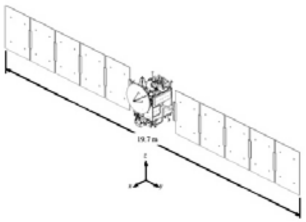

DAWN trajectory

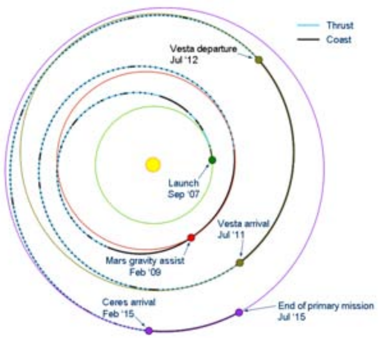

Vesta as seen by DAWN

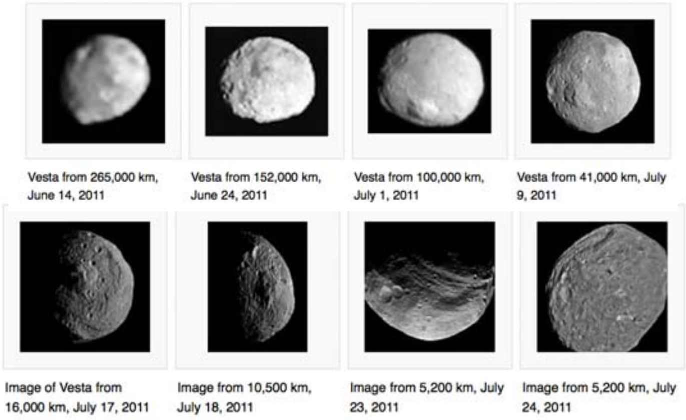

HED meteorites

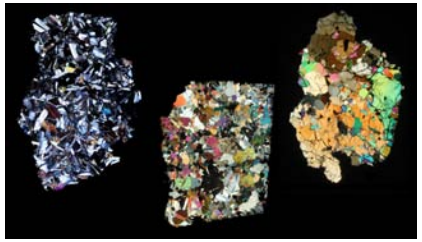

This image shows three slices of ahowardite, eucrite and diogenite meteorites that the Dawn mission has confirmed as originating from the giant asteroid Vesta. The meteorites are viewed through a polarizing microscope, where different minerals appear in different colors. The texture of the rocks reveals that they crystallized at different rates. The image on the left comes from a meteorite named QUE 97053 (Antarctica), which is basaltic eucrite. The image in the middle comes from the Moore County (North Carolina) cumulate eucrite. The image on the right comes from a diogenite meteorite named GRA 98108 (Antarctica).

Vestas global distribution of craters

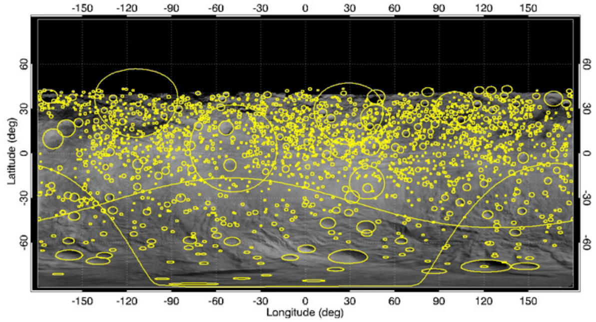

This graphic shows the global distribution of craters that hit the giant asteroid Vesta, based on data from NASA's Dawn mission. The yellow circles indicate craters of (4 kilometers or wider, with the size of the circles indicating the size of the crater. The two huge impacts in the southern hemisphere appear as undulating lines in this projection.

Meteorites - Asteroids

Are meteorites pieces of astroids?

If yes, why are the spectral characteristics so different?

And how did the meteorites get from the Astroidebelt to Earth?